

Processing and Morphology of Molecularly Imprinted Nylon Thin Films

Asta Richter,¹ Ursula J. Gibson,² Marek Nowicki,³ Joseph J. BelBruno²

¹Department of Engineering Physics, University of Applied Sciences Wildau, 15754 Wildau, Germany

²Center for Nanomaterials Research, Dartmouth College, Hanover, New Hampshire 03755

³Institute of Physics, Poznan University of Technology, 60-965 Poznan, Poland

Received 12 January 2005; accepted 30 September 2005

DOI 10.1002/app.23369

Publication online in Wiley InterScience (www.interscience.wiley.com).

ABSTRACT: The characterization of thin, selectively imprinted films of nylon-6 was performed. Amino acids were used as template molecules. Spin-cast films were prepared with sizes ranging from 2 μm to 300 nm, depending on the nylon and template concentration in the casting solution. The morphological characteristics of the film surface were examined by atomic force microscopy, and the structure within the films was observed by freeze-fracture scanning

electron microscopy. The film activity was clearly coordinated with the appearance of nanometer-sized pores both on the surface and within the film. © 2006 Wiley Periodicals, Inc. *J Appl Polym Sci* 101: 2919–2926, 2006

Key words: molecular imprinting; spin coating; morphology; atomic force microscopy; scanning electron microscopy

INTRODUCTION

Molecular imprinting is a chemical technique for the production of molecule-specific cavities that mimic the behavior of natural receptor binding sites without the temperature sensitivity and high cost of the natural systems.^{1–3} Artificial polymers may be built for any target molecule. Molecularly imprinted polymers (MIPs) are typically prepared^{4,5} by polymerization in the presence of a template molecule that interacts with the polymer network via bonding interactions or intermolecular forces. The template is subsequently removed, but the template binding site remains and the polymer exhibits the ability to recognize the template with a high degree of selectivity. The most common applications of MIPs have been chromatographic separations of drugs or biological products.^{6,7} Powdered chromatography packing materials are generated to analyze small quantities of material.

More recently, one research group in Japan^{8,9} and a second in Italy¹⁰ have turned to the study of MIP porous membranes as components of purification devices to remove contaminants from solutions of biological materials. These membranes are prepared by a phase-inversion technique that involves using poly-

merized starting material dissolved with the template in a theta solvent, and then the membrane is cast by immersion in a nonsolvent to solidify the polymer.

We recently reported on an improved nylon-based MIP that employed formic acid as the solvent.¹¹ In this phase-inversion-like procedure, the material is created from polymer pellets and the polymerization step, which has inherent chemical difficulties due to incomplete and side reactions, is eliminated. Our variant on this procedure, which we term the *solvent crystallization technique*, followed the initial steps of the phase-inversion procedure¹² in that polymer pellets and the template molecule are dissolved simultaneously and allowed to interact in solution to form the imprint. Unlike the phase-inversion method, in which the polymer solution is spread manually over a large area with a thickness of 10s or 100s of microns and then solidified by immersion in water (which does not solvate the polymer), we spin cast our films directly onto the substrate. The films are produced by the rapid evaporation of the theta solvent leading to semicrystallization of the polymer with amorphous inclusions. Both the polymer network and the templated polymer network are held together by intermolecular hydrogen bonds.^{13,14} These bonds are used to create the recognition sites that later act as receptors for the template molecule. A recent article also used the spin-coating method to control film thickness.¹⁵

The templating process may be summarized as follows. When dissolved in formic acid solution, the crystalline nylon polymer is separated into elongated chains. These chains form a hydrogen-bonded network in solution. The template molecules are added to

Correspondence to: J. J. BelBruno (joseph.j.belbruno@dartmouth.edu).

Contract grant sponsor: DAAD.

Contract grant sponsor: National Science Foundation; contract grant numbers: D/0247265 and INT-0233261.

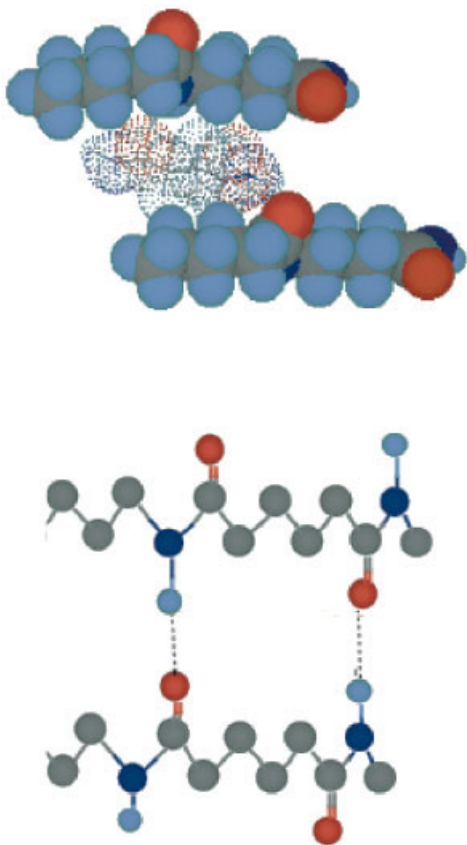


Figure 1 A schematic representation of the template molecule within the nylon host. Color codes: black is carbon, light blue is hydrogen, red is oxygen, and dark blue is nitrogen. (top) A space filling model of the template hydrogen bonded in nylon and (bottom) a molecular structure model showing the hydrogen-bonded nylon without the template. Because the template has the same amide functionality as nylon, it hydrogen bonds in the same manner (e.g., nitrogen-bound hydrogen from nylon to the carbonyl oxygen of the amino acid). [Color figure can be viewed in the online issue, which is available at www.interscience.wiley.com]

this solution at room temperature and crosslink the nylon chains via hydrogen bonds. This is a slow process at room temperature, but the lower temperature is preferable to heating the sample and increasing the likelihood of template molecule decomposition. The amino acids were superior to nylon itself as hydrogen-bonding agents. Figure 1 provides a two-dimensional schematic representation of the formation of the template receptor site. The figure shows only the monomer occupation of a binding site and does not include the additional nylon molecules that surround the template. These have been omitted for clarity. Spin coating evaporates the solvent, forming a thin film that is a mixture of crystalline and amorphous nylon. The thickness is primarily a function of the weight percentage of polymer in the casting solution; however, the presence of the template molecule does contribute to the film thickness.

The advantage of this technique, in addition to controlled thickness, is the potential for processing these films as active elements in sensors. If a MIP-based sensor is developed to function as one component of a chip, that device must be processed like any normal circuit, including coating and etching processes. For sensor applications, the accessibility of the templated sites to the analyte is critically important. This is determined by a combination of the thickness of the film and the diffusion coefficient of the analyte through the film. The latter is critically dependent on the microstructure of the film. In a previous article¹⁶ we described the surface morphology containing apparent pores in the surface. In this work, we expand upon those measurements and reveal that the pore structure is present throughout the film. We describe the physical characterization of the MIP system, including the film thickness and surface/bulk morphology, by means of atomic force microscopy (AFM) and freeze-fracture scanning electron microscopy (SEM).

EXPERIMENTAL

Nylon-6 was obtained from Aldrich (3-mm pellets, melting temperature = 276°C), formic acid (99%) was Fisher Scientific reagent grade, and the amino acids used as template molecules were obtained from Sigma. Solutions composed of 10 mL of formic acid with up to 20 wt % nylon pellets and up to 10 wt % amino acid were covered (but not air purged) and stirred at room temperature for 24 h. Films were spin cast from these solutions onto 18-mm square glass microscope cover slips. The slides were prewashed in concentrated nitric acid and cleaned with spectroscopic grade isopropanol and acetone prior to polymer deposition. The spin coater was operated at 4000 rpm for 30 s, with negligible ramp-up time. Control samples were produced without amino acid templates. IR spectra were used to determine the presence or absence of the template molecule. Typically, FTIR spectra were recorded over a narrow region of interest at 3600–2000 cm^{-1} for the NH stretch or 1750–1550 cm^{-1} in the carbonyl region. Film thickness was measured using a Tencor Instruments Alpha Step 500 stylus profilometer and a Micro-Xam surface mapping microscope. Optical microscopy and SEM measurements of the film thickness were in agreement with those from the profilometer.

AFM was performed on a Digital Instruments Nanoscope 3 scanning probe microscope in contact mode. Electron micrographs were recorded on a Zeiss DSM 962 SEM microscope after freezing in liquid nitrogen and fracture of the substrate with the film.

RESULTS AND DISCUSSION

The results that follow involve selected amino acids, alanine, and L-glutamine as the template molecules.

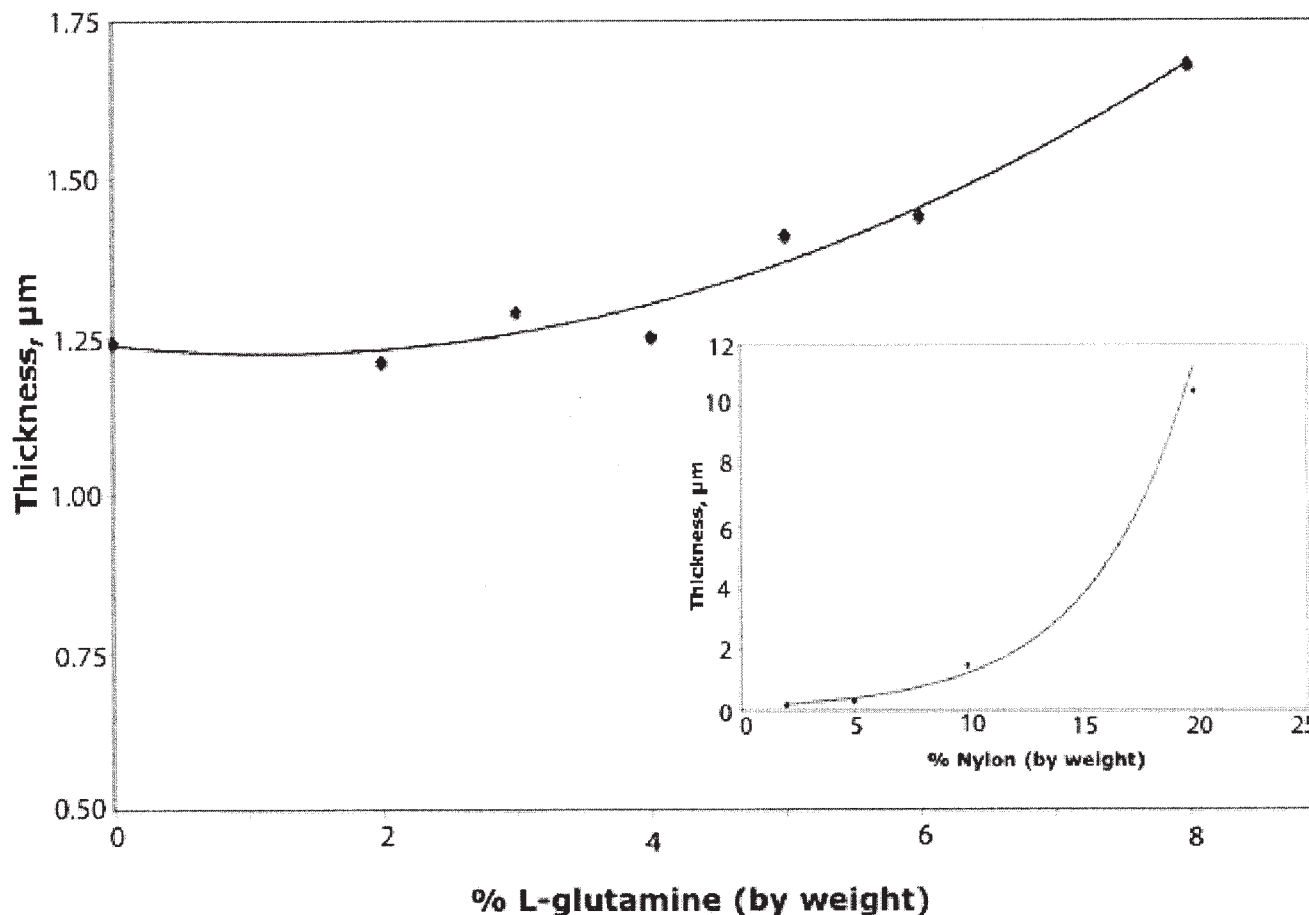


Figure 2 The film thickness as a function of the weight percentage of template molecules (L-glutamine) and weight percentage of nylon (inset) in the casting solution. All thicknesses are from at least five different films with calculated standard deviations of approximately 2%.

However, films produced from other amino acids (*R*-glutamine, histidine, tryptophan, serine, cysteine, or aspartic acid) exhibited film thicknesses and morphologies similar to those reported here.

Deposition thickness

Control over film thickness is critical for future applications of MIPs, because the film is usually combined with a surface-sensitive transducer element. We report the parameters that control the film thickness in our system. Profilometry and surface mapping were used to measure the thickness of the films. The process of spin coating is a balance between the viscosity of the coating solution and the evaporation of the solvent. The nature of the polymerization is dependent on the speed of the solvent evaporation. The relationship between the concentrations of the MIP components and film thickness was examined by the variation of both the nylon and template concentrations. The combined results are shown in Figure 2. The concentration of nylon in the casting solution was the dominant variable. The film thickness increased rapidly with

increasing nylon concentration. At the lowest concentrations, the practical limitation on the minimum film thickness is adhesion to the substrate. The film thickness is less dependent on the concentration of the template molecule in the casting solution, but it nevertheless increased with increasing amino acid concentration. This is an intriguing result. Simple optical microscopy indicated a finer granular structure within the films as the concentration of template molecules was increased. These granular features are indicative of inhomogeneous evaporation of the solution. The presence of amino acids, which are excellent hydrogen-bonding agents, may trap solvent molecules and slow the film-casting process, resulting in a more uniform surface. In this model, nucleation begins as the solvent evaporates during spin casting. Evaporation increases the effective concentration of nylon and solution semicrystallization occurs with large regions of amorphous material trapped within each granule. Higher concentrations of template provide more effective hydrogen bonding among nylon chains and lead to a finer scale structure in the evaporated film.

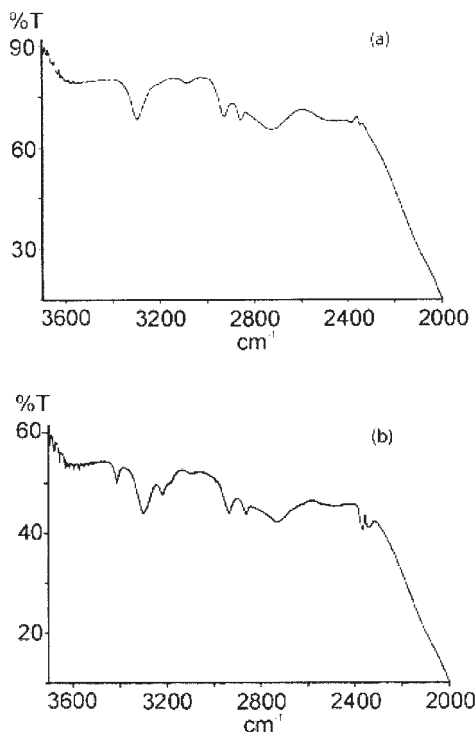


Figure 3 IR spectra in the —NH stretching region of (a) a control nylon film from a 5% nylon solution and (b) a templated nylon film produced from a 5% L-glutamine/5% nylon solution. Samples were stirred continuously for 24 h prior to spin casting. The casting parameters are described in the text. Prewashed slides were coated at 4000 rpm for 30 s.

Chemical characterization

The chemical nature of the MIPs and their interaction with the nylon host were examined by IR spectroscopy. The amino acid concentrations are sufficiently small and the nylon host acts so effectively as an immobilization agent that the template molecules are spectroscopically isolated, as they would be in a cryogenic matrix. Narrow absorption bands result and the transitions due to the amino acids may easily be resolved from those of the nylon host, even though the absorptions from both the MIP and the control are due to analogous —NH or carbonyl stretches. Typical IR spectra are shown in Figure 3. The spectra in the —NH stretching region for both the control sample produced from a 5% nylon solution and the MIP sample from a 5% nylon plus 5% L-glutamine solution are shown. The spin-coating conditions were as described in the Experimental section. The presence of the template molecule is clearly indicated by the additional band in Figure 3(b). Similar changes in the IR spectrum are observed for other amino acid template molecules. The films exhibit template concentration ratios of approximately 0.35. That is, regardless of the chemical identity of the amino acid, its concentration within the film, which is calculated from the IR spectrum, is

typically 35% of the concentration in the casting solution.

Imprint specificity

Reddy et al.¹² demonstrated the specificity of a powdered form of the identical L-glutamine imprinted polymer, and we previously published related data involving films.¹¹ The powdered imprinted polymer binding studies indicated that the imprinted material exhibited a 4:1 preference for L-glutamine over D-glutamine.¹² Our samples are thin films rather than granulated samples and whereas the uptake for the film may be less than for an equivalent quantity of powdered polymer because of the surface area of the latter, there is no reason to suspect a variation in the measured specificity. As confirmation, we explored the reintroduction of L-glutamine into a 1 μm thick spin-coated film using IR spectroscopy. This technique is not the most sensitive procedure for accurate re-binding studies. However, it is sufficient to confirm the specificity of the product and, because our goal in this work is to examine the morphology as a function of the state of the film, our need is to show the presence or absence of the target molecule and the absence of any foreign species. We previously reported similar results for thin imprinted films.¹¹ The film was initially imprinted with L-glutamine and subsequently removed as described above. Reintroduction was conducted by immersion of the film in a 150-mM solution of L-glutamine in 5% formic acid for variable amounts of time. In the case of L-glutamine, the band corresponding to the NH stretch of the amino acid at $\sim 3400\text{ cm}^{-1}$ indicated a reinsertion to approximately 80% of

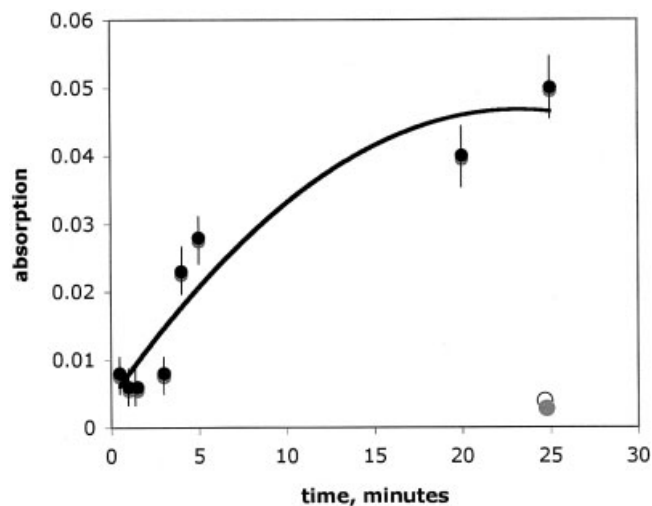


Figure 4 The IR absorption intensity at 3400 cm^{-1} (amino acid NH stretching frequency) as a function of the amino acid reintroduction time into an L-glutamine imprinted film from which the amino acid was extracted: (●) L-glutamine, (○) L-arginine, and (○) nylon control.

the concentration of the initially prepared film after 30-min immersion. The results of these absorption measurements are shown in Figure 4. Identical experiments, using a control (unimprinted polymer film) or L-arginine (similar size and chemical properties as L-glutamine) as the amino acid, resulted in no observable absorption, as indicated in the figure. This result is not meant to infer that no L-arginine was taken up into the film. Rather, the level that was introduced into the L-glutamine imprinted film was below the detection limit of our method. These results exclude the possibility of surface adsorption of the amino acid on nylon. We conclude that the film specificity is unchanged from the granulated imprinted polymer specificity and proceed to examine the morphology differences in the imprinted, extracted, amino acid reintroduced, and control materials.

Film topography

In our previous studies we confirmed that receptor sites are created in MIPs. The surface roughness and pore distribution in MIP films varies with the template molecules.¹⁶ Our goal here is to examine the nature of these binding sites from a topological perspective. To that end, the morphological features of the deposited films were analyzed by both freeze-fracture SEM to examine the interior and AFM to explore the surface properties. It is worth noting that SEM images of imprinted *membranes* (not films) of much greater thickness ($\sim 10\text{--}100\ \mu\text{m}$) are available in the literature¹⁰ and AFM images^{17,18} of MIPs and sol-gel imprints¹⁹ have been reported, but few direct AFM images of the imprint sites have been published previously. To our knowledge, this is the first correlation of the surface

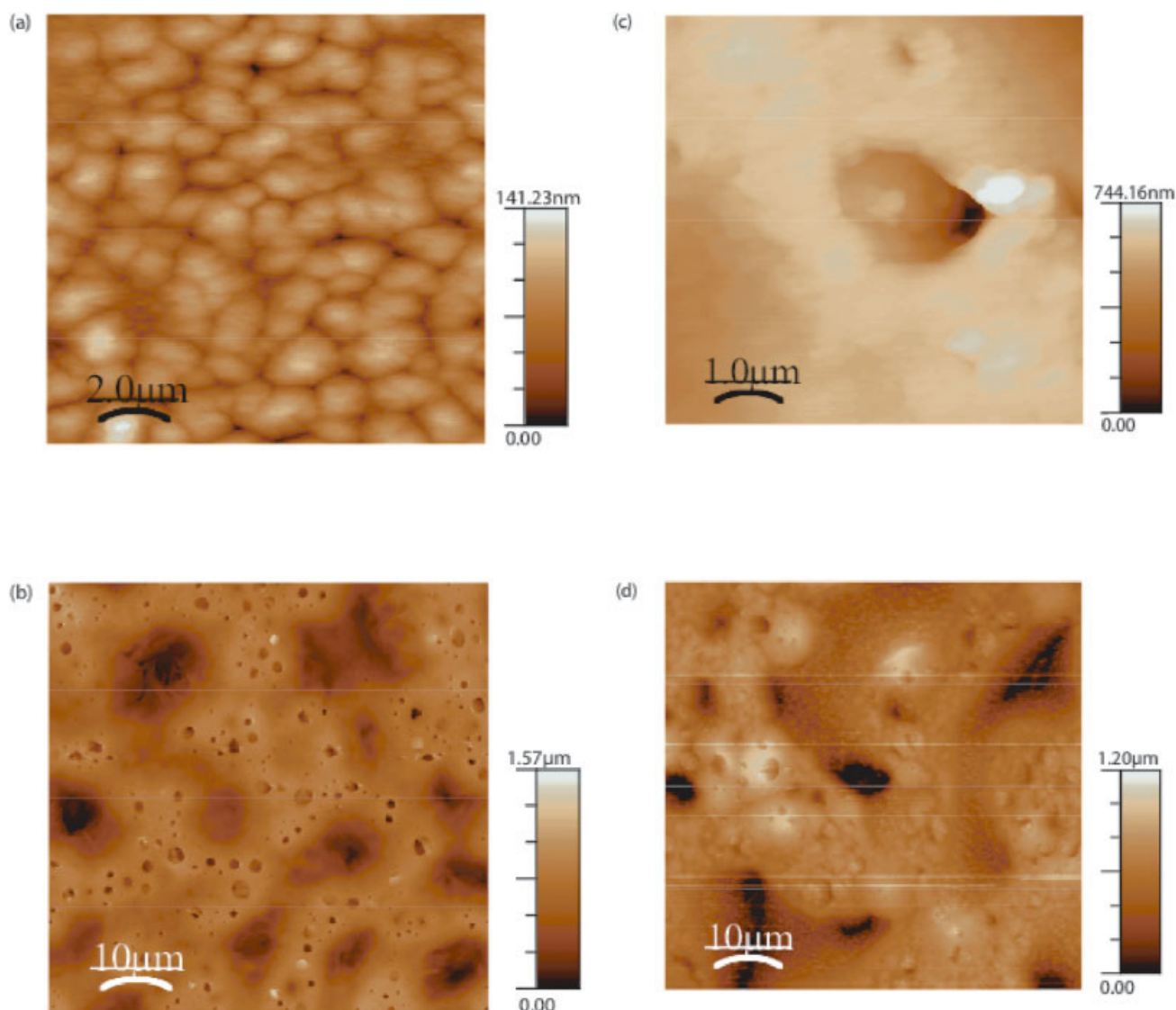


Figure 5 An AFM image of (a) 5% nylon control film, (b) lower magnification L-glutamine imprinted nylon thin film, (c) higher magnification L-glutamine imprinted nylon thin film, and (d) lower magnification alanine imprinted nylon thin film. [Color figure can be viewed in the online issue, which is available at www.interscience.wiley.com]

and bulk structure of MIP films using a combination of these techniques.

The AFM results on a $10 \times 10 \mu\text{m}$ 5% nylon control film are provided in Figure 5(a). A slightly lower magnification ($50 \times 50 \mu\text{m}$) AFM image of an L-glutamine imprinted 5% polymer film ($\sim 800 \text{ nm}$ thick) is shown in Figure 5(b). The imprinted film surface has numerous depressions without patterned regularity. The low magnification image of the imprinted film shows a wide distribution of pore dimensions. A qualitative scan of Figure 5(b) indicates a relative pore diameter distribution density ratio of $0.06 : 0.09 : 0.33 : 0.41 : 1.0$ for $\sim 5\text{-}\mu\text{m}$, $\sim 2\text{-}\mu\text{m}$, $\sim 1\text{-}\mu\text{m}$, $\sim 400\text{-nm}$, and $\sim 100\text{-nm}$ diameters, respectively. The $\sim 100\text{-nm}$ diameter pores occur at least twice as frequently as any other pore size. However, the higher magnification image in Figure 5(c) indicates that the largest openings ($1\text{--}5 \mu\text{m}$) are only associated with the top surface of the film; the pore narrows as it enters into the bulk of the film. Alanine imprinted (5% nylon) films have a different overall surface morphology as may be seen in Figure 5(d). Although the range of pore diameters is similar, the distribution across the surface differs; there is a greater number of the larger diameter pores. The pores are formed during the solidification process of the polymer films via evaporation of the solvent during spin coating. This process results in different pore structures and pore size distributions that reflect the different hydrogen-bond strengths of the template molecules. Most importantly, the pores are only present when the template is included in the nylon film. That is, no pores or channels are observed in a control film, such as that shown in Figure 5(a).

Chemical swelling is employed both to remove template molecules after the formation of the film and to later use the films to bind analyte molecules from solution. The amino acid may be removed from the intact film by washing in a 5% formic acid solution for 2 min and may be reintroduced by an analogous process, which includes 5 wt % amino acid in the formic acid solution. An AFM image of an L-glutamine imprinted (5% nylon) film, from which the template has been removed and L-glutamine subsequently reintroduced, is shown in Figure 6. This image confirms that the surface morphology is not modified by the removal/reintroduction of the amino acid template. Moreover, if one attempts to reintroduce a "foreign" amino acid that was not used to imprint the film, the surface morphology remains unchanged. It is the initial imprinting process that determines the postextraction morphology.

The imprinting process clearly alters the surface morphology in comparison to the control sample by producing pores and channels, but we have not addressed the question of porosity within the entire film: can analyte molecules reach receptor sites in the interior of the thin film? To examine the interior of the

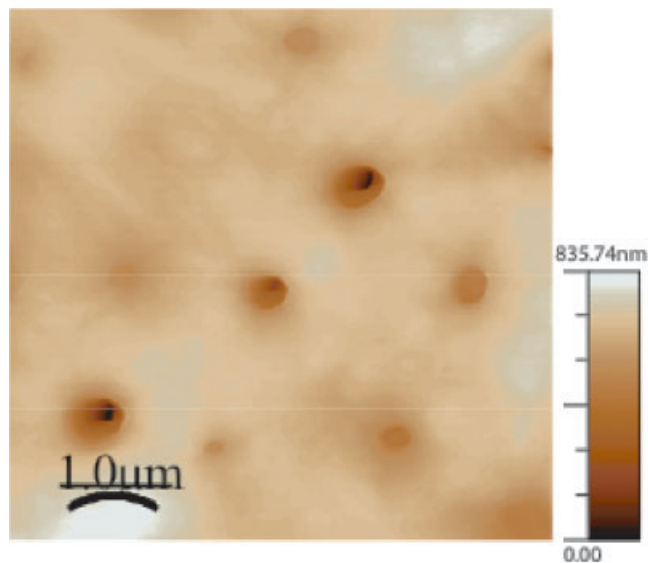


Figure 6 An AFM image of a 5% L-glutamine imprinted nylon film from which the glutamine was removed and subsequently reintroduced. [Color figure can be viewed in the online issue, which is available at www.interscience.wiley.com]

films, the freeze-fracture SEM technique was used. Figure 7 images both a control and an imprinted film at an angle of 30° after fracture at 77 K. The control in the bottom picture in the figure has a relatively smooth surface with no pores. The film is 870 nm thick as measured at the fracture face. There is no evidence of a membranelike or porelike structure in this micrograph. In contrast, the top of the figure contains a similarly fractured and imaged L-glutamine imprinted film, estimated to be 900 nm thick. The top surface is seen to contain the same pores that were more distinctly imaged in AFM. The fractured edge, which is actually a view of the interior of the film, contains pores whose diameters on the fractured surface are in the range of 10s of nanometers. The large channels observed on the surface are not observed in the interior of the films. In general, the average diameters of the pores within the interior of the film are smaller than those measured on the surface by AFM. However, in the interior of the film, these diameters represent the full size of the pores rather than their surface apertures and we noted that the surface pores decrease in diameter with decreasing depth into the film. The important piece of information extracted from the SEM image is that the imprint process has occurred throughout the film and not simply on the surface. Transport to receptor sites can occur through the top apertures or more slowly through the polymer network.

The template molecules are typically on the order of 1 nm in length, which is quite different from the size of the pores observed in our films. The additional

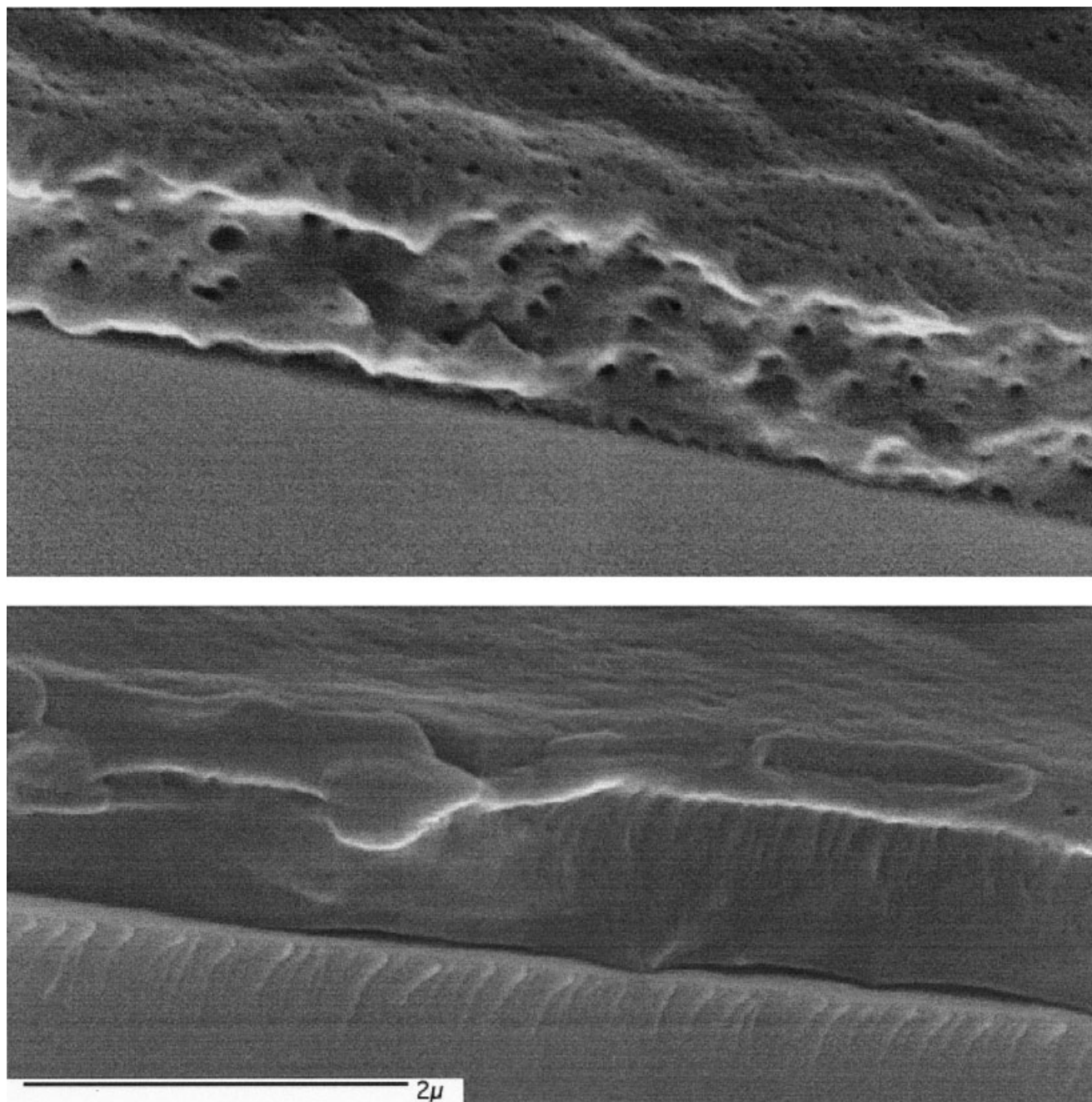


Figure 7 A comparison of freeze-fracture SEM images of (top) control nylon and (bottom) L-glutamine imprinted nylon films.

volume of the measured pores results in part from the geometrical form of the template molecule and the arrangement of that molecule within the polymer host. This may be seen from space filling models such as that shown in Figure 1. The inclusion of only two of the many nylon host molecules surrounding the template glutamine increases the overall width of the system shown in the figure to approximately 2 nm. The smallest of the cavities we observed are on the order of this diameter, but many are much larger. We attribute the larger pores to clustering of the template molecule in solution.

CONCLUSIONS

The phase-inversion/spin-casting process described here opens up new semiconductor-compatible processing techniques for combining MIP films with sensor elements. We presented information on the pore structure and connectivity in nylon films imprinted with amino acids. AFM and freeze-fracture SEM are effective techniques for the direct study of the surface and internal structure of imprinted thin films. Analyses of the images from these two techniques provided detailed information on the film thickness

and the pore dimensions of the films. Pores of approximately 70-nm diameter were produced throughout the $\sim 1 \mu\text{m}$ thick nylon film when a template molecule was present during film spin casting. These images were direct observations of the active receptor sites in MIPs.

The authors thank Dr. Charles Daghljan for assistance with the SEM imaging of the films. We gratefully acknowledge the support of DAAD and the National Science Foundation.

References

1. Shea, K. J. *Trends Polym Sci* 1994, 2, 166.
2. Wulff, G. *Angew Chem Int Ed* 1995, 34, 1812.
3. Mosbach, K.; Ramstrom, O. *Biotechnology* 1996, 14, 163.
4. Das, K.; Duff, D. J.; Hsu, S. L.; Penelle, J.; Rotello, V. M. *Polym Prepr* 2000, 41, 1173.
5. Yan, M.; Kapua, A. *Polym Prepr* 2000, 41, 264.
6. Owens, P. K.; Karlsson, L.; Lutz, E. S. M.; Anderson, L. I. *Trends Anal Chem* 1999, 18, 146.
7. Ensing, K.; deBoer, T. *Trends Anal Chem* 1999, 18, 138.
8. Wang, H. Y.; Kobayashi, T.; Fukaya, T.; Fuhii, N. *Langmuir* 1997, 13, 5396.
9. Shibata, M.; Kobayashi, T.; Fuhii, N. *J Appl Polym Sci* 1999, 75, 1546.
10. Trotta, F.; Drioli, E.; Baggiani, C.; Lacopo, D. *J Membr Sci* 2002, 201, 77.
11. Shneshkoff, N.; Crabb, K.; BelBruno, J. J. *J Appl Polym Sci* 2002, 86, 3611.
12. Reddy, P. S.; Kobayashi, T.; Fuhii, N. *Chem Lett* 1999, 293.
13. Sreenivasan, K.; Sivakumar, R. *J Appl Polym Sci* 1999, 71, 1823.
14. Yoshida, M.; Uezo, K.; Goto, M.; Furusaki, S. *J Appl Polym Sci* 2000, 78, 695.
15. Schmidt, R. H.; Mosbach, K.; Haupt, K. *Adv Mater* 2004, 16, 719.
16. Maier, P.; Werner-Allen, J.; Gibson, U. J.; Richter, A.; BelBruno, J. J. *Surf Interface Anal* 2004, 36, 134.
17. Hilal, N.; Kochkodan, V.; Al-Khatib, L.; Busca, G. *Surf Interface Anal* 2002, 33, 672.
18. Yoshimi, Y.; Ohdaira, R.; Iiyama, C.; Sakai, K. *Sens Actuators B* 2001, 73, 49.
19. Dickert, F. L.; Hayden, O. *Anal Chem* 2002, 74, 1302.